Research Square

Preprints are preliminary reports that have not undergone peer review.
They should not be considered conclusive, used to inform clinical practice,
or referenced by the media as validated information.

Comparative Performance Analysis of 2D Materials Based Surface Plasmon Resonance Sensor for HST6 Gastric Cancer Cell Detection

Raina Ranjan
Veer Kunwar Singh University Ara
Akhil Kumar Mishra
Veer Kunwar Singh University Ara
Nitish Kumar
Veer Kunwar Singh University Ara
Alpana Shrivastava
Sri Shankar College Sasaram (Constituent Body of Veer Kunwar Singh University Ara)
Sushil Kumar
skumarmaurya85@gmail.com

Sri Shankar College Sasaram (Constituent Body of Veer Kunwar Singh University Ara)

Research Article

Keywords: surface plasmon resonance, 2D materials. sensitivity, detection accuracy, figure of merit, HST6 gastric cancer

Posted Date: September 2nd, 2026

DOI: https://doi.org/10.21203/rs.3.rs-10772790/v1

License: This work is licensed under a Creative Commons Attribution 4.0 International License.
Read Full License

Additional Declarations: No competing interests reported.

Version of Record: A version of this preprint was published at Journal of Computational Electronics on October 20th, 2026. See the published version at https://doi.org/10.1007/s10825-026-02657-7.

Comparative Performance Analysis of 2D Materials Based Surface Plasmon Resonance Sensor for HST6 Gastric Cancer Cell Detection

Raina Ranjan[1], Akhil Kumar Mishra[1], Nitish Kumar[1], Alpana Shrivastava[2] and Sushil Kumar[3]

[1]Department of Physics, Veer Kunwar Singh University Ara, Bihar, India,802301

[2]Department of Botany, Sri Shankar College Sasaram (Constituent Body of Veer Kunwar Singh University Ara), Rohtas, Bihar 821115, India

[3]Department of Physics, Sri Shankar College Sasaram (Constituent Body of Veer Kunwar Singh University Ara), Rohtas, Bihar 821115, India

Abstract:

Surface plasmon resonance based biosensors have attracted considerable attention for rapid, label-free, and highly sensitive biomedical detection. In the present study, a comparative investigation of five two-dimensional (2D) materials namely graphene, molybdenum disulfide (MoS_2), tungsten disulfide (WS_2), hexagonal boron nitride (h-BN), and black phosphorus (BP) is presented using a multilayer SPR configuration. Initially, the sensing performance of each 2D material was systematically evaluated over a sensing medium refractive index range of 1.330-1.335 RIU. The sensing characteristics of SPR sensor are analysed in terms of resonance angle, sensitivity, full width at half maximum (FWHM), detection accuracy (DA) and figure of merit (FOM). The results demonstrate that the sensing performance is strongly influenced by the optical properties of the incorporated 2D material with BP exhibiting the most favourable overall sensing characteristics. Based on this comparative analysis, the optimized BP integrated SPR sensor was further investigated for the detection of HST6 Gastric Cancer cells. The optimized SPR sensor achieved a maximum sensitivity of 419.27°/RIU, FWHM of 5.1360°, DA of 0.1947 deg^{-1} and FOM of 81.63 RIU^{-1}. This result demonstrates the potential of the proposed BP based SPR sensor as a promising platform for HST6 Cancer detection.

Keywords: surface plasmon resonance, 2D materials. sensitivity, detection accuracy, figure of merit, HST6 gastric cancer.

Correspond to:

Dr. Sushil Kumar
Department of Physics,
Sri Shankar College Sasaram,
Rohtas, Bihar-821115, India
Mobile No. +918077741207
e-mail : skumarmaurya85@gmail.com

1. Introduction

Surface plasmon resonance (SPR) sensors have attracted considerable attention in recent years because of their high sensitivity, real-time monitoring capability, and label-free detection mechanism. SPR occurs due to the interaction of p-polarized light with free electrons present at a metal-dielectric interface, producing surface plasmons that are highly sensitive to refractive index variations near the sensing layer [1]. Because of these advantages, SPR sensors are widely used in chemical sensing, medical diagnostics, environmental monitoring, and biomolecular detection. In the early development of SPR sensors based on noble metals such as gold (Au) and silver (Ag) were widely studied using the Kretschmann configuration. Gold has good chemical stability and biocompatibility, whereas silver offers sharper resonance curves and better optical performance. However, conventional metal-based SPR sensors have some drawbacks such as oxidation of silver, broad resonance curves, lower detection accuracy, and limited sensitivity, which restrict their performance in high-precision biosensing applications [2]. To improve the sensing performance, researchers have introduced 2D materials like as graphene into SPR structures because of its excellent electrical conductivity, large surface area, and strong adsorption ability for biomolecules. Therefore, Graphene-based SPR sensors can provide better sensitivity and biomolecular interaction compared to conventional metallic structures [3]. However, graphene has a zero bandgap and relatively weak light absorption, which can limit its performance in some optical sensing applications [4]. To overcome the limitations of graphene, transition metal dichalcogenides (TMDC) such as MoS_2 and WS_2 have been widely explored. These materials possess tunable bandgap, high optical absorption, and strong interaction with light, making them promising candidates for SPR biosensors [5]. MoS_2 based SPR sensors can improve sensing performance because of the useful optical properties of MoS_2. However, the thickness and number of MoS_2 layers should be optimized to obtain better sensitivity and detection accuracy [6,7]. Similarly, WS_2 has emerged as another important material for SPR enhancement due to its larger adsorption efficiency and stronger electromagnetic field confinement. Kumar et al. reported that WS_2 based SPR sensors provide better sensitivity than graphene and MoS_2 based structures because of improved light absorption and plasmonic interaction [8] However, increasing the number of WS_2 layers can broaden the SPR resonance and reduce the detection accuracy; therefore, the WS_2 layer thickness should be carefully optimized [9]. Apart from TMDCs, BP has also been explored for SPR sensing, and BP-based structures can improve the sensitivity of conventional SPR sensors [10]. However, black phosphorus is chemically unstable under ambient environmental conditions and undergoes rapid degradation when exposed to oxygen and moisture, limiting its practical applicability [11]. h-BN has attracted attention in SPR sensing because of its useful dielectric properties and high stability. The addition of h-BN can improve the sensitivity and overall performance of SPR sensors [12]. However, h-BN absorbs less light than TMDC materials. Therefore, it may not improve the SPR sensor sensitivity as much [13].

In present work, our aim to provide deeper insights into the role of various 2D materials in enhancing SPR sensing performance. Although several studies have reported SPR enhancement using individual 2D materials such as graphene, MoS_2, WS_2, h-BN and BP but a systematic comparative investigation of these materials under identical multilayer SPR

configurations is still limited. Therefore, a comprehensive comparative analysis of SPR sensor performance is carried out by incorporating these prominent 2D materials into a multilayer configuration. The sensing performance of each 2D materials systematically evaluated in term of sensitivity, FWHM, DA and FOM parameter to identify the most suitable 2D material for enhancing SPR sensor performance. Thereafter, the multilayer SPR structure incorporating the best-performing 2D material is further optimized for the detection of HST6 gastric cancer cells and its sensing performance is evaluated. This paper is organized as follows: section 2 describes the theoretical modelling and design of the SPR sensor. Section 3 presents numerical simulation results and discussion along with their comparison. Finally, the conclusions of the study are summarized in Section 4.

2. Theoretical Model of SPR Sensor:

Surface plasmon waves (SPW) are excited when the propagation constant of the incident p-polarized light matches the wave vector of the surface plasmon mode at the metal-dielectric interface. This phase matching condition leads to the excitation of SPR. The SPR condition can be expressed as [1]:

$$\frac{2\pi}{\lambda} n_p sin\theta = \frac{2\pi}{\lambda} \sqrt{\frac{\varepsilon_m \varepsilon_s}{\varepsilon_m + \varepsilon_s}} \tag{1}$$

where n_p is the refractive index of the coupling prism, λ is the free space wavelength, ε_m and ε_s are dielectric constants of the metal and sensing medium respectively. The resonance condition is satisfied when the wave vector component of the incident light matches the propagation constant of the surface plasmon wave vector, resulting in efficient energy transfer from the incident optical field to the SPW. At the resonance angle, maximum coupling of the incident optical energy to the surface plasmon mode occurs, resulting in a pronounced minimum in the reflected light intensity. Any variation in the refractive index (RI) of the sensing medium alters the phase-matching condition and consequently induces a shift in the resonance angle. This resonance shift constitutes the fundamental sensing mechanism of the proposed SPW biosensor. The theoretical investigation of the proposed SPW biosensor is performed using the transfer matrix method (TMM) a well-established and versatile approach for analysing multilayer SPR configurations. In the N-layer model, each constituent layer is characterized by its complex dielectric permittivity and thickness. The TMM establishes the relationship between the tangential components of the electric and magnetic fields at the boundaries of the multilayer structure, thereby enabling the calculation of the reflectance spectrum and resonance characteristics of the proposed SPR configuration. For p-polarized incident light, the characteristic matrix of the k^{th} layer is expressed as [14]:

$$M_k = \begin{bmatrix} cos\beta_k & -\frac{i}{q_k} sin\beta_k \\ -iq_k sin_k & cos\beta_k \end{bmatrix} \tag{2}$$

Where

$$\beta_k = \frac{2\pi d_k}{\lambda} \sqrt{(\epsilon_k - n_p^2 sin^2\theta)} \tag{3}$$

and

$$q_k = \frac{\sqrt{(\epsilon_k - n_p^2 sin^2\theta)}}{\epsilon_k} \quad (4)$$

Here β_k represents the phase thickness and d_k represents the thickness of the k^{th} layer, θ is the angle of incidence and ϵ_k denotes the k^{th}layer of dielectric constant of the corresponding layer and n_p denote the refractive index of the coupling prism. The total characteristic matrix of the multilayer structure is obtained as:

$$M = \prod_{k=2}^{N-1} M_k \quad (5)$$

The reflection coefficient for p-polarized light is expressed as:

$$r = \frac{[(m_{11} + m_{12}q_N)q_1 - (m_{21} + m_{22}q_N)]}{[(m_{11} + m_{12}q_N)q_1 + (m_{21} + m_{22}q_N)]} \quad (6)$$

The reflectance intensity of the SPR structure is given by:

$$R = |r|^2 \quad (7)$$

The performance of the proposed SPR sensor is evaluated using sensitivity, FWHM, DA and FOM [15]: The sensitivity of the SPR sensor is defined as:

$$S = \frac{\Delta\theta_{res}}{\Delta n_s} \quad (8)$$

where $\Delta\theta_{res}$ is the shift in resonance angle and Δn_srepresents the refractive index variation of the sensing medium. The detection accuracy of the SPR sensor is defined as:

$$DA = \frac{1}{FWHM} \quad (9)$$

where FWHM is the full width at half maximum of the SPR reflectance curve. The quality factor of the sensor is given by:

$$FOM = \frac{S}{FWHM} \quad (10)$$

3. Results and Discussion:

The proposed multilayer SPW based sensor is designed using the Kretschmann configuration and schematically illustrated Fig.1. The proposed structure consists of a coupling prism, an adhesive layer, plasmonic metallic layer, dielectric enhancement layer, 2D material layer and sensing medium. In this configuration, p-polarized monochromatic light is incident through the coupling prism at a particular wavelength to excite surface plasmon waves at the metal-dielectric interface. A BK7 glass prism is employed as the coupling medium owing to its excellent optical transparency and suitable refractive index for efficient coupling of incident light to the surface plasmon mode. A thin ZnO layer is introduced between the prism and the metallic layer to enhance interfacial adhesion and modify the local

electromagnetic field distribution. Ag is selected as the plasmonic metal layer because of its favourable optical properties, strong plasmonic response, and relatively sharp resonance characteristics compared with gold. To further enhance the electromagnetic field confinement at the sensing interface, a $BaTiO_3$ dielectric enhancement layer is used into the proposed structure. Subsequently, a thin layer of a selected 2D material (graphene, MoS_2, WS_2, h-BN, and BP) is deposited on the $BaTiO_3$ layer to improve biomolecule absorption and strengthen plasmonic interaction with the analyte. The RI of each layer of constituent layer is listed in table1. The thicknesses of the ZnO, and Ag layers are fixed at 10 nm, and 50 nm, respectively based on values reported in previous studies that demonstrated favourable sensing performance [16,17]. The proposed multilayer structure is numerically simulated using the TMM with each selected 2D materials individually and systematically evaluate its sensing performance parameter. The corresponding RI and thickness of the investigated 2D materials are summarized in table 2.

The reflectance curve of the proposed SPR multilayer waveguide for a single graphene layer of thickness 0.34 nm are shown by the blue curve in fig.2. As the RI of sensing medium increases from 1.330 to 1.335, the resonance dip shifts toward a higher incident angle, confirming the RI sensing capability of proposed SPR structure. The resonance angle shifts from 71.49 to 72.22 corresponding to an angular shift of 0.73. For this single graphene layer, the calculated sensitivity, FWHM, DA and FOM are 145.72°/RIU, 2.10°, 0.47 deg^{-1}, and 69.09 RIU^{-1}, respectively. To investigate the influence of the number of the graphene layer, the number of graphene layers is systematically increased from 1 to 10. The corresponding sensing parameters obtained for different numbers of graphene layers are summarized in table 3. The reflectance curve corresponding to ten graphene layers is also presented by the red curve in fig.2.The maximum sensitivity is achieved 182.36°/RIU for the 10-layer graphene configuration which is higher the previously reported research papers [18,19-21]. From the table, it is observed that the sensitivity increases gradually with an increase in the number of graphene layers. However, the DA decreases significantly from 0.4742 $deg^{-1}$to 0.1055deg^{-1} due to broadens the resonance curve and reduces the sharpness of the resonance dip. Consequently, the FOM decreases from 69.0953RIU^{-1} to 19.2333RIU^{-1} as the number of graphene layers increases. Therefore, this result indicates that although multilayer graphene improves sensitivity but excessive graphene layers deteriorate the detection accuracy and overall sensing quality. Similar calculation has been done upto 10 layers MoS_2 but the better performance is observed at the 3 layers of MoS_2 layer. The reflectance curve for 3 layers is also shown in fig.3(a). The optimised sensitivity, FWHM, DA, FOM is 193.96°/RIU, 10.33°, 0.09deg^{-1}, 18.75RIU^{-1} respectively. The obtained sensitivity is higher than that reported previously for MoS_2 based waveguide sensors [6,18,22,]. The reflectance spectra of the proposed SPR waveguide consist MoS_2 layers are presented in fig.3(a). For a single MoS_2 layer, the resonance angle shifts from 72.80° to 73.59° as the RI of the sensing medium increases, resulting in an angular shift of 0.79°. The corresponding sensitivity, FWHM, DA and FOM are 158.36°/RIU, 3.53°, 0.28 deg^{-1}, and 44.76 RIU^{-1}, respectively. To investigate the effect of the number of MoS_2, the number of layers is varied from 1 to 10. The calculated sensing performance parameters for different numbers of MoS_2 layers are summarized in table 4. Among the investigated configurations, the three layers of MoS_2 structure exhibits the most favourable overall sensing performance. The obtained sensitivity is higher than that reported in previous studies on MoS_2 based SPR waveguide sensors, demonstrating the potential of the proposed configuration for high sensitivity RI sensing. The effect of WS_2

layers on the SPR sensing performance is presented in Fig.3(b). The blue curve considers as one layer of WS_2, whereas the red curve shows the response obtained with 3 layers of WS_2. For the single WS_2 layer, the resonance angle changes from 73.21° to 74.03°, giving a sensitivity of 163.28°/RIU. The corresponding FWHM, DA, and FOM are 2.57°, 0.38deg^{-1}, and 63.43 RIU^{-1}, respectively. To find the suitable number of WS_2 layers, the calculation was performed by varying the layers from 1 to 10. Among them, 3 layers of WS_2 give better sensing performance. At 3 layers, the obtained sensitivity, FWHM, DA, and FOM are 274.78°/RIU, 7.25°, 0.13deg^{-1}, and 37.86RIU^{-1}, respectively. Hence, three WS_2 layers are considered suitable for the proposed sensor. Fig.3(c) shows the SPR curve for h-BN layers. The blue curve represents the single h-BN layer, while the red curve represents the optimized 10 h-BN layers. For the single h-BN layer, the resonance angle shifts from 71.32° to 72.04° and the calculated sensitivity, FWHM, DA, and FOM are 144.04°/RIU, 1.65°, 0.60 deg^{-1}, and 87.18RIU^{-1} respectively. The number of h-BN layers is increased up to 10 layers and it was found that the sensor gives better performance with 10 layers. For 10 layers h-BN, the sensitivity, FWHM, DA, and FOM are 167.12°/RIU, 2.06°, 0.48 deg^{-1} and 80.85RIU^{-1} respectively. Therefore 10 h-BN layers are selected as the optimized structure for further analysis. The reflectance curve for the BP based sensor is shown in fig.3(d). For a single layer of BP, the calculated sensitivity, FWHM, DA, and FOM are 149.64°/RIU, 1.77°, 0.56 deg^{-1}and 84.10 RIU^{-1} respectively. The resonance angle shifts from 71.90° to 72.65° for the change in sensing medium refractive index. The same analysis was carried out by increasing the BP layers up to 10. Among all the cases, better performance was obtained with 8 layers of BP. The reflectance curve for 8 BP layers is also shown in fig.3(d). The sensitivity, FWHM, DA, and FOM for 8 layers of BP are 380.48°/RIU, 4.63°, 0.21 deg^{-1}, and 82.10 RIU^{-1}, respectively. The results show that the sensitivity increases when the number of BP layers is increased from 1 to 8 layers.

The sensing performance parameters obtained for a single layer and the optimized number of layers of each 2D materials are summarized in table 5. The results demonstrate that the different 2D materials significantly influences the sensitivity, FWHM, DA and FOM of the proposed SPR sensor. Among the investigated configurations, the BP based structure exhibits the highest sensitivity of 380.48°/RIU with 8 BP layers, whereas the h-BN based waveguide provides the highest FOM of 87.18 RIU^{-1} and the highest detection accuracy of 0.60 deg^{-1} for a single layer. These results indicate that the choice and number of 2D material layers play a crucial role in determining the sensing characteristics and overall performance of the proposed multilayer SPR configuration. Table 6 presents a comparative analysis of the sensitivity achieved by the proposed SPR sensor with those reported for previously investigated 2D materials based SPR configurations. The enhanced sensitivity can be attributed to the combined effects of ZnO dielectric layer, Ag metallic layer, $BaTiO_3$ dielectric enhancement layer and the high optical and surface interaction characteristics of the 2D materials. These results demonstrate the potential of the proposed multilayer architecture for achieving enhanced refractive-index sensitivity compared with conventional 2D material based SPR configurations. The proposed multilayer SPR sensor was further optimized by varying the thickness of each constituent layer to achieve the highest sensing performance for HST6 Gastric cancer cell detection. The refractive indices of 1.360 and 1.371 were considered for normal and cancerous HST6 cells respectively[28]. The optimized sensor configuration consisted of a 8 nm ZnO layer, 43 nm Ag layer, 2 nm $BaTiO_3$ layer, and 8 layers of BP. The corresponding reflectivity spectra of the optimized multilayer SPR sensor

are presented in Fig. 4. The SPR reflectance curves exhibit a distinct shift in the resonance angle when the refractive index changes from normal to cancerous HST6 cells. This resonance angle shift demonstrates the capability of the proposed sensor to effectively discriminate between healthy and malignant HST6 cells. The optimized sensor achieves a maximum sensitivity of 419.27°/RIU, indicating its excellent ability to detect small changes in the refractive index associated with HST6 cancer cells. Furthermore, the sensor exhibits a FWHM of 5.1360°, DA of 0.1947deg^{-1}, and FOM of 81.63 RIU^{-1}. These performance parameters further confirm the high sensing quality and potential of the proposed multilayer SPR configuration for sensitive gastric cancer detection.

4. Conclusion:

A comparative analysis of graphene, MoS_2, WS_2, h-BN, and BP assisted multilayer SPR sensors was presented. The influence of number of 2D material layers on the sensing performance has been investigated in terms of sensitivity, FWHM, DA and FOM. The results confirm that the sensing characteristics are strongly dependent on the optical properties and thickness of the incorporated 2D material. Among the different 2D materials, BP demonstrated the highest sensitivity of 380.48°/RIU with 8 BP layers, whereas h-BN exhibited the highest FOM of 87.1807 RIU^{-1} and detection accuracy of 0.6053 deg^{-1} for a single layer. Based on this comparative assessment, the BP integrated SPR structure was further optimized for HST6 cancer detection by optimizing the thicknesses of the constituent layers. The optimized sensor exhibited a pronounced resonance angle shift and achieved a maximum sensitivity of 419.27°/RIU, FWHM of 5.1360°, DA of 0.1947 deg^{-1} and FOM of 81.63 RIU^{-1}. The proposed BP based multilayer SPR sensor therefore provides an improved platform for highly sensitive and label free discrimination of normal cells and HST6 cancer cells. The systematic comparison of different 2D materials further establishes a useful design framework for selecting and optimizing 2D materials in SPR biosensors.

Acknowledgment:

The authors are thankful to Prof. Abhay Kuamr Singh and Prof. Vivek Singh, Department of Physics, Banaras Hindu University, Varanasi for their continuous encouragement.

References:

[1] Homola J.: Surface plasmon resonance sensors for detection of chemical and biological species. Chemical Reviews 108(2), 462-493 (2008)

[2] Maier S.A.: Plasmonics: Fundamentals and Applications. Springer, New York, (2007)

[3] Bonaccorso F., Sun Z., Hasan T., Ferrari A.C.: Graphene photonics and optoelectronics. Nature Photonics 4,611-622 (2010)

[4] Geim A.K., Novoselov K.S.: The rise of graphene. Nature Materials 6(3),183-191 (2007)

[5] Wang Q.H., Kalantar-Zadeh, K., Kis A., Coleman J.N., Strano M.S.: Electronics and optoelectronics of two-dimensional transition metal dichalcogenides. Nature Nanotechnology 7,699-712 (2012)

[6] Srivastava A., Prajapati Y.K.: Performance analysis of silicon and blue phosphorene/MoS_2 hetero-structure based on SPR sensor. Photonic Sensors 9(3) ,284-292 (2019)

[7] Ouyang Q., Zeng S., Jiang L., Hong L., Xu G., Dinh X.Q., Qian J., He S., Qu J., Coquet P., Yong K.T.: Sensitivity enhancement of transition metal dichalcogenides/silicon nanostructure-based surface plasmon resonance biosensor. Scientific Reports 6, 28190 (2016)

[8] Kumar A., Yadav A.K., Kushwaha A.S., Srivastava S.K.: A comparative study among WS_2, MoS_2 and graphene-based surface plasmon resonance (SPR) sensor. Sensors and Actuators Reports 2(1), 100015 (2020)

[9] D. Wang J. Liu H. Yang B. Huang, and G. Zeng.: Research on tunable SPR sensors based on WS_2 and graphene hybrid nanosheets. Photonics 9(7), 490 (2022)

[10] T. Srivastava and R. Jha.: Black phosphorus. A new platform for gaseous sensing based on surface plasmon resonance. IEEE Photonics Technology Letters 30(4), 319-322 (2018)

[11] Qiao J., Kong X., Hu Z.X., Yang, F., Ji, W.: High-mobility transport anisotropy and linear dichroism in few-layer black phosphorus. Nature Communications 5, 4475 (2014)

[12] H. Zheng, J. Yang, Q. Wang, B. Feng, R. An.: Sensitivity enhancement of fibre surface plasmon resonance (SPR) sensor based upon a gold film-hexagonal boron nitride-molybdenum disulfide structure. Instrumentation Science & Technology 50(6), 589-603 (2022)

[13] Zhi C., Bando Y., Tang C., Golberg D.: Boron nitride nanotubes. Materials Science and Engineering: R: Reports 70(3-6), 92-111 (2010)

[14] B. Gupta, A.K. Sharma.: Sensitivity evaluation of a multi-layered surface plasmon resonance-based fiber optic sensor: a theoretical study, Sensors and Actuators B: Chemical 107 ,40-46 (2005)

[15] Panda A., Pukhrambam P.D.: Modeling of high-performance SPR refractive index sensor employing novel 2D materials for detection of malaria pathogens. IEEE Transactions on Nanobioscience, 21(2), 312–319 (2022)

[16] Paliwal A., Gaur R., Sharma A., Tomar M., Gupta V.: Sensitive optical biosensor based on surface plasmon resonance using ZnO/Au bilayered structure. Optik 127(19), 7642-7647 (2016)

[17] Uddin, S.M.A., Chowdhury, S.S., Kabir, E.: Numerical analysis of a highly sensitive surface plasmon resonance sensor for SARS-CoV-2 detection. Plasmonics 16, 2025-2037 (2021)

[18] Kumar A, Yadav AK, Kushwaha AS, Srivastava SK (2020) A comparative study among WS_2, MoS_2 and graphene based surface plasmon resonance (SPR) sensor. Sensors and Actuators Reports 2(1) ,100015 (2020)

[19] Verma R., Gupta B.D., Jha R.: Sensitivity enhancement of a surface plasmon resonance based biomolecules sensor using graphene and silicon layers. Sensors and Actuators B: Chemical 160(1), 623-631 (2011)

[20] Lin C., Chen S.: Design of high-performance Au-Ag-dielectric-graphene based surface plasmon resonance biosensors using genetic algorithm. Journal of Applied Physics 125, 113101 (2019)

[21] Maharana P.K., Padhy P., Jha R.: On the field enhancement and performance of an ultra-stable SPR biosensor based on graphene. IEEE Photonics Technology Letters 25(22), 2156-2159 (2013)

[22] J. Maurya, Y. Prajapati, V. Singh, J. Saini, R. Tripathi.: Performance of graphene–MoS 2 based surface plasmon resonance sensor using silicon layer, Optical and Quantum Electronics 47 ,3599-3611 (2015)

[23] Banerjee J., Ray M.: Comparative performance evaluation of mono-metallic and bimetallic plasmonic sensors using WS_2 and graphene with optical bio-sensing application. Sensors and Actuators B: Chemical 281, 520-526 (2019)

[24] Al-Haraidh W.S., Ahmed M.F.: 2D-layers coupled with metal nitrides as efficient plasmonic materials in surface plasmon resonance sensor: Gold-level performance and urine glucose detection. Journal of King Saud University -Science 37, 12792025 (2025)

[25] R. Kumar, S. Garia, S. Joshi, A. Pal, I. Singh, and U. K. Sahu.: A high-performance SPR biosensor for female reproductive hormone detection. IEEE Access 13, 86057-86068 (2025)

[26] Srivastava A., Verma A., Das R., Prajapati Y.K.: A theoretical approach to improve the performance of SPR biosensor using MXene and black phosphorus. Optik 203, 163430 (2020)

[27] J.B. Maurya, A. François, Y.K. Prajapati.: Two-dimensional layered nanomaterial-based one-dimensional photonic crystal refractive index sensor, Sensors 18 ,857 (2018)

[28] Paiva J.S., Jorge P.A.S., Ribeiro R.S.R., Balmaña M., Campos D., Mereiter S., Jin, C., Karlsson N.G., Sampaio P., Reis C.A., Cunha J.P.S.: iLoF: An intelligent Lab on Fiber Approach for Human Cancer Single-Cell Type Identification. Scientific Reports 10, 3171 (2020)

[29] Yadav A., Kumar S., Malomed B.A.: Enhancing bimetallic SPR sensor's performance: The role of 2D and TMDC nanomaterials. Plasmonics 20(7), 4985-4996 (2025)

[30] Zhu Q., Shen Y., Chen Z., Chen B., Dai E., Pan W.: Anisotropic sensing performance in a high-sensitivity surface plasmon resonance sensor based on few-layer black phosphorus. Sensors 24(12), 3851 (2024)

[31] A. Paul, K. Rishav, G. Klootwijk, M. Sarkar, O. Bisht, Z. Li, S. Conesa-Boj, G. T. Papadakis, and S. F. Pereira.: Characterization of the 3D-Optical Properties of van der Waals Materials with Deep Learning-Based Coherent Fourier Scatterometry. ACS Photonics 13(1), 224-235 (2026)

[32] Y. Hattori, T. Taniguchi, K. Watanabe.: Antireflection Substrates for Determining the Number of Layers of Few-Layer Hexagonal Boron Nitride Films and for Visualizing Organic Monolayers. ACS Applied Nano Materials 6, 21876-21886 (2023)

[33] Fouad S., Sabri N., Jamal Z.A.Z., Poopalan P.: Enhanced sensitivity of surface plasmon resonance sensor based on bilayers of silver-barium titanate. Journal of Nano- and Electronic Physics 8(4(2)) ,04085 (2016).

Statements & Declarations

Funding:

No funding was received for conducting this study.

Conflicts of interest/Competing interests:

The authors have no conflicts of interest to declare that are relevant to the content of this article.

Data availability:

No datasets were generated or analysed during the current study.

Contributions:

Raina Ranjan: Conceptualization, Original draft preparation, Visualization, **Akhil Kumar Mishra:** Simulation, **Nitish Kumar:** Data Analysis, Validation, **Alpana Shrivastava:** Review and Editing, **Sushil Kumar:** Supervision

Table:1 RI of the constituent layers of the proposed SPR sensor.

Table:2 RI and Thickness of the each 2D Materials of the proposed SPR sensor.

Table:3 Effect of the number of graphene layers on the performance parameters of the proposed SPR sensor.

Table:4 Effect of the number of MoS_2 layers on the performance parameters of the proposed SPR sensor.

Table:5 Comparison of the sensing performance parameters of the proposed SPR sensor for single and optimized numbers of 2D material layers.

Table 6. Comparison of the sensitivity of the proposed SPR sensor with previously reported 2D material based SPR sensors.

Fig.1 Schematic diagram of the SPR Sensors.

Fig.2 Reflectance of the proposed SPR sensor for one and ten layers of graphene.

Fig.3(a) Reflectance of the proposed SPR sensor for one and three layers of MoS_2.

Fig.3(b) Reflectance of the proposed SPR sensor for one and three layers of WS_2.

Fig.3(c) Reflectance of the proposed SPR sensor for one and ten layers of h-BN.

Fig.3(d) Reflectance of the proposed SPR sensor for one and eight layers of BP.

Fig.4 Reflectance of the proposed SPR sensor for normal and cancerous HST6 gastric cancer cells.

Table:1

Layer	RI	Reference
ZnO	1.952+0.02i	[16]
Ag	0.059+4.243i	[19]
Sensing medium	1.330-1.335	[29]
BK7	1.515	[30]
BaTiO3	2.4043	[33]

Table:2

2D Materials	RI	Thickness(nm)	Reference
Graphene	3+1.1491i	0.34	[27]
MoS_2	5.0947+1.2327i	0.65	[27]
WS_2	4.8937+0.3124i	0.80	[27]
Black Phosphorus	3.50+0.01i	0.53	[29]
h-BN	2.10+0i	0.33	[31,32]

Table:3

Number of graphene layer	Sensitivity (°/RIU)	FWHM (°)	DA (deg^{-1})	FOM (RIU^{-1})
1	145.72	2.1090	0.4742	69.0953
2	149.60	2.6666	0.3750	56.1014
3	153.76	3.2904	0.3039	46.7299
4	158.16	3.9853	0.2509	39.6858
5	162.76	4.7550	0.2103	34.2292
6	167.48	5.6000	0.1786	29.9071
7	172.12	6.5150	0.1535	26.4190
8	176.48	7.4856	0.1336	23.5759
9	180.08	8.4865	0.1178	21.2195
10	182.36	9.4820	0.1055	19.2333

Table:4

Number of MoS_2 layer	Sensitivity (°/RIU)	FWHM (°)	DA (deg^{-1})	FOM (RIU^{-1})
1	158.36	3.5374	0.2827	44.7673
2	180.02	6.5437	0.1528	27.5104
3	193.96	10.3391	0.0967	18.7599
4	140.90	13.0308	0.0767	10.8128
5	57.56	14.7710	0.0677	3.8968
6	19.26	16.5509	0.0604	1.1637
7	5.64	18.3611	0.0545	0.3072
8	0.92	20.1186	0.0497	0.0457
9	0.40	21.2385	0.0471	0.0188
10	0.30	21.0240	0.0476	0.0143

Table:5

2D Martials	Number of 2D layer	Maximum sensitivity (°/RIU)	FWHM (°)	DA (deg^{-1})	FOM (RIU^{-1})
Graphene	1	145.72	2.1090	0.4742	69.0953
	10	182.36	9.4820	0.1055	19.2333
MoS2	1	158.36	3.5374	0.2827	44.7673
	3	193.96	10.3391	0.0967	18.7599
WS2	1	163.28	2.5734	0.3886	63.4359
	3	274.78	7.2571	0.1378	37.8636
h-BN	1	144.04	1.6522	0.6053	87.1807
	10	167.12	2.0669	0.4838	80.8554
BP	1	149.64	1.7792	0.5621	84.1052
	8	380.48	4.6343	0.2158	82.1009

Table:6

2D Material	SPR Sensor Structure	Sensitivity	Reference
Graphene	BK7-ZnO-Ag-$BaTiO_3$-Graphene	157.00	[18]
	BK7-Au-Si-Graphene	134.60	[19]
	BK7-Au-Ag-TiO_2-Graphene	100.00	[20]
	BK7-Ag (48 nm)-Graphene	97.76	[21]
	BK7-ZnO-Ag-$BaTiO_3$-Graphene (10 layers)	182.36	Present work
MoS_2	Prism-Au-Blue Phosphorus-MoS_2	159.33	[6]
	BK7-ZnO-Ag-$BaTiO_3$-MoS_2	174.00	[18]
	Prism-Au-Si-MoS_2-Graphene	48.65	[22]
	BK7-ZnO-Ag-$BaTiO_3$-MoS_2 (3 layers)	193.96	Present work
WS_2	Prism-Au-Si-WS_2	147.88	[7]
	BK7-ZnO-Ag-$BaTiO_3$-WS_2	180.00	[18]
	Prism-Ag-WS_2-Graphene	126.33	[23]
	BK7-ZnO-Ag-$BaTiO_3$-WS_2 (3 layers)	274.78	Present work
h-BN	Prism-ZrN-h-BN	140.04	[24]
	SF11-Cu-Pd-h-BN	97.24	[25]
	BK7-ZnO-Ag-$BaTiO_3$-h-BN (10 layers)	167.12	Present work
BP	BK7-TiN-BP	149.50	[24]
	BK7-Au-MXene-BP	184.49	[26]
	BK7-Au-MXene-WS2-BP	190.22	[26]
	BK7-ZnO-Ag-$BaTiO_3$-BP (8 layers)	380.48	Present work

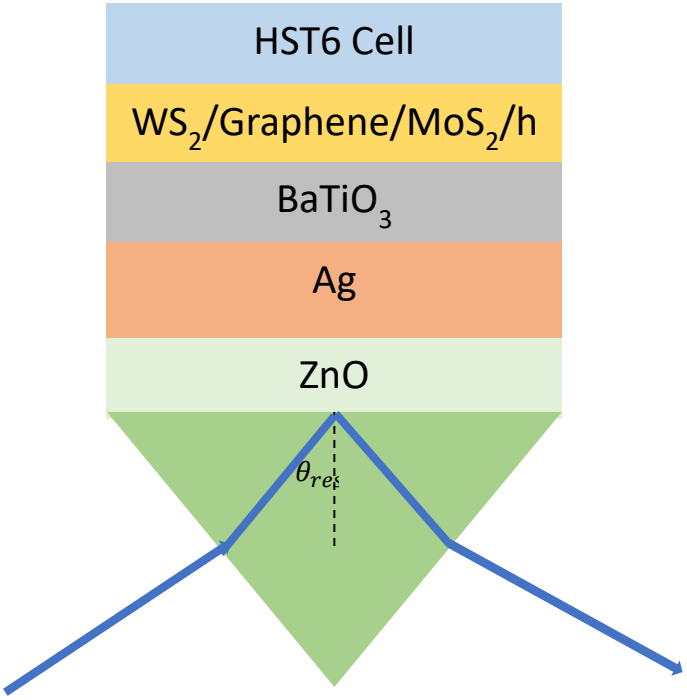


Fig.1

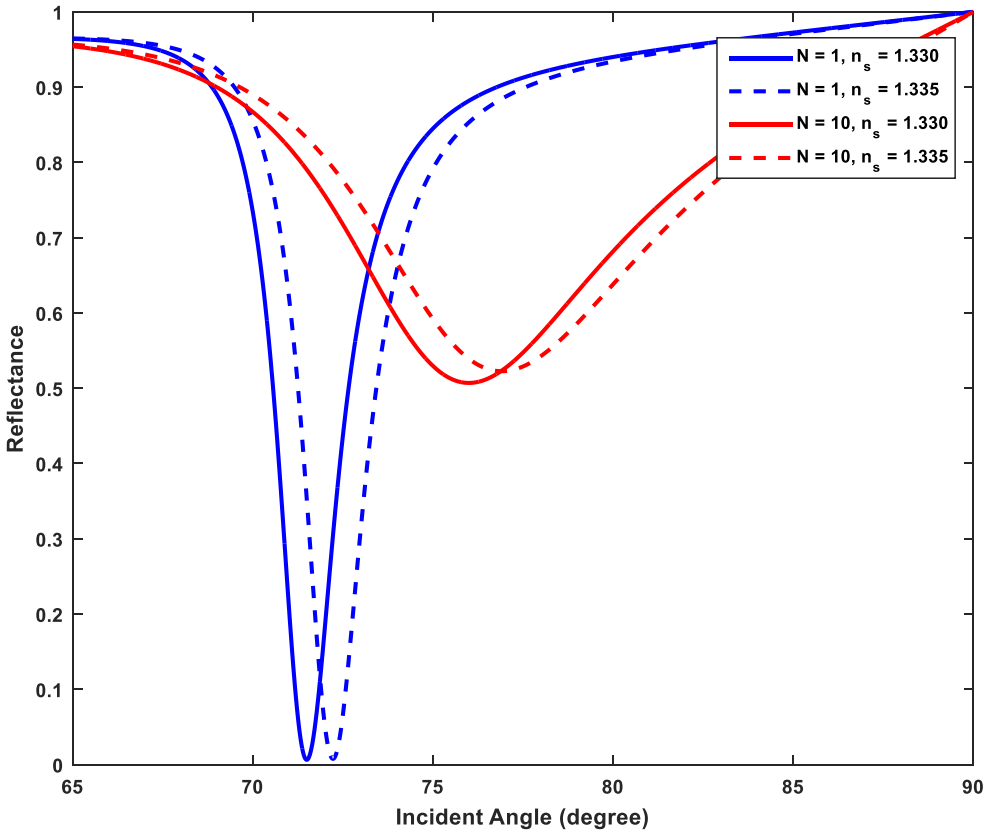

Reflectance
Incident Angle (degree)
N = 1, n_s = 1.330
N = 1, n_s = 1.335
N = 10, n_s = 1.330
N = 10, n_s = 1.335
0
0.1
0.2
0.3
0.4
0.5
0.6
0.7
0.8
0.9
1
65
70
75
80
85
90

Fig.2

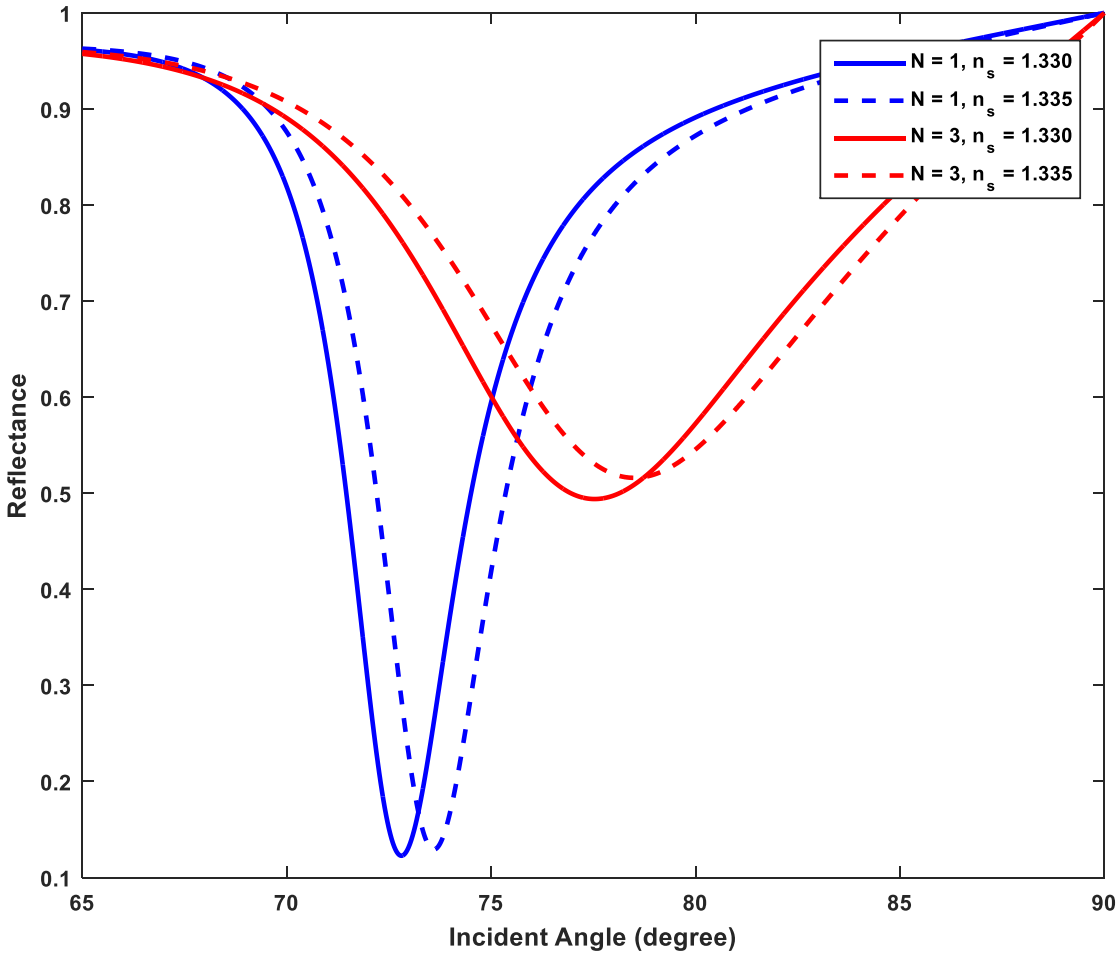

Reflectance
Incident Angle (degree)
N = 1, n_s = 1.330
N = 1, n_s = 1.335
N = 3, n_s = 1.330
N = 3, n_s = 1.335
1
0.9
0.8
0.7
0.6
0.5
0.4
0.3
0.2
0.1
65
70
75
80
85
90

Fig.3(a)

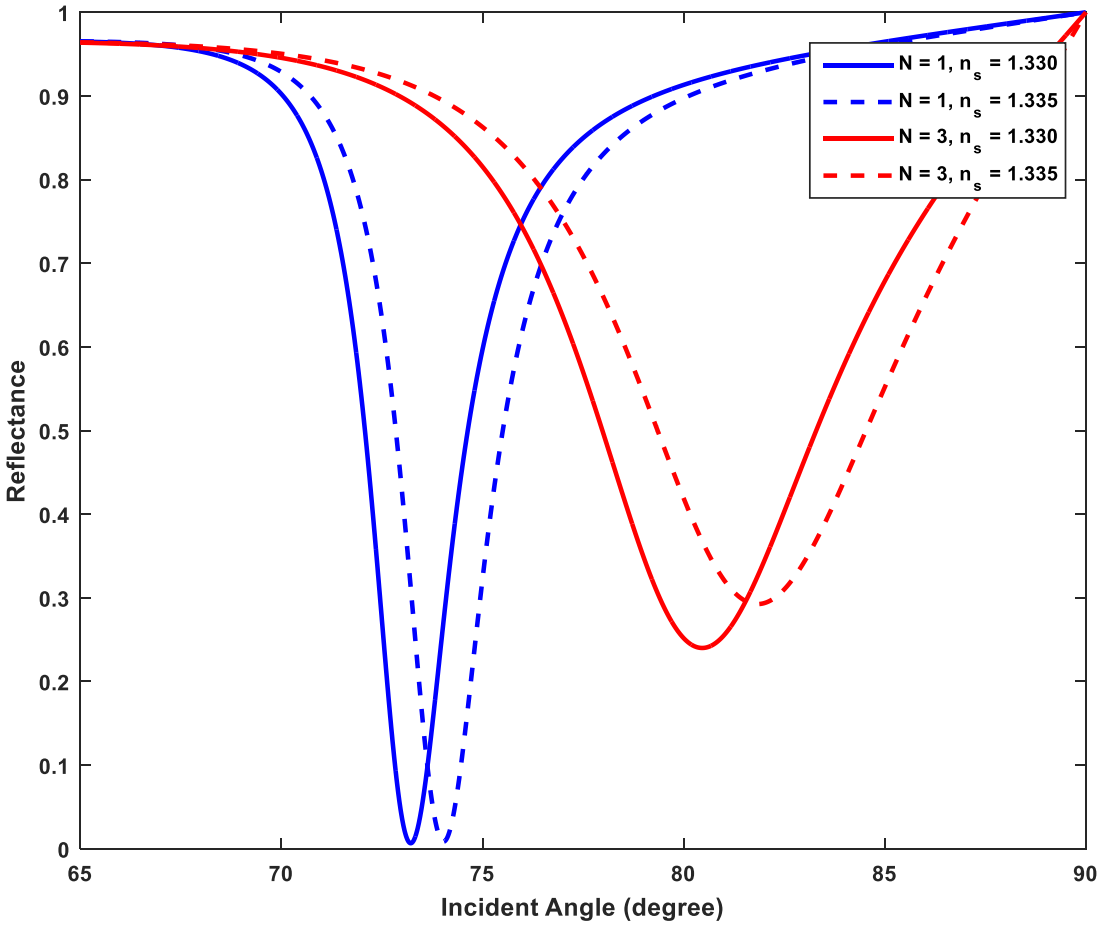

Reflectance
Incident Angle (degree)
N = 1, n_s = 1.330
N = 1, n_s = 1.335
N = 3, n_s = 1.330
N = 3, n_s = 1.335
0
0.1
0.2
0.3
0.4
0.5
0.6
0.7
0.8
0.9
1
65
70
75
80
85
90

Fig.3(b)

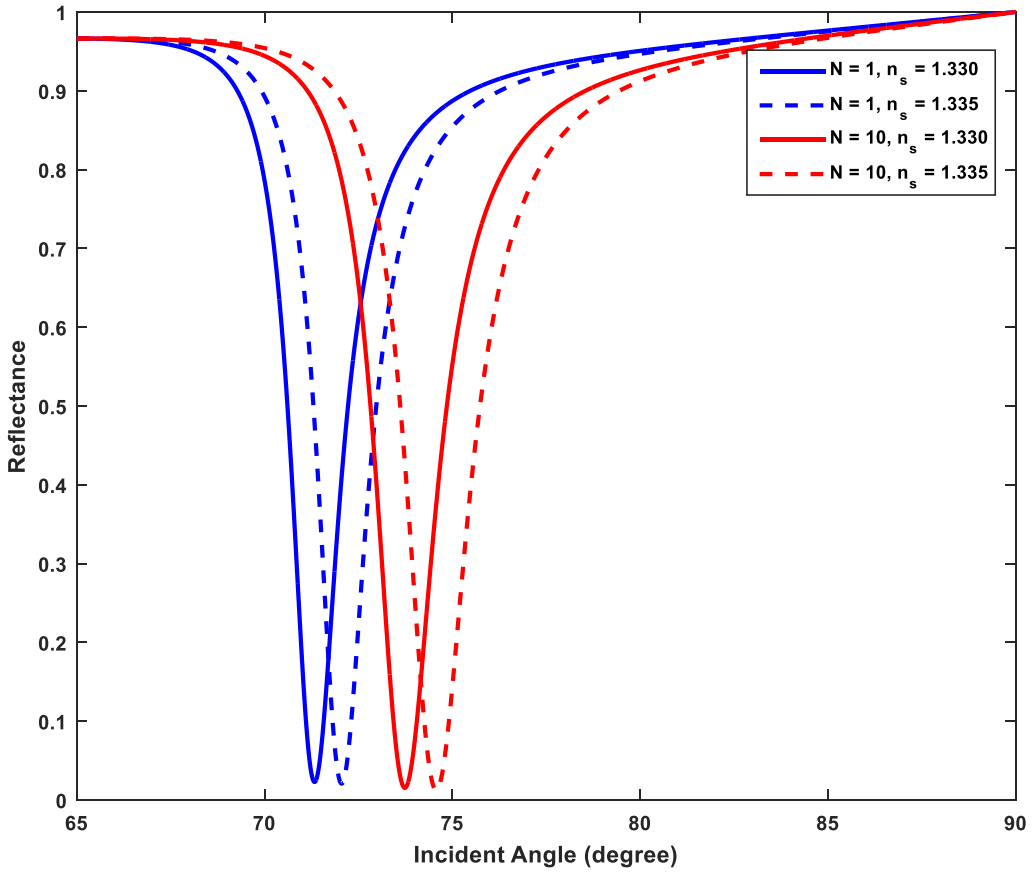

Reflectance
Incident Angle (degree)
N = 1, n_s = 1.330
N = 1, n_s = 1.335
N = 10, n_s = 1.330
N = 10, n_s = 1.335
0
0.1
0.2
0.3
0.4
0.5
0.6
0.7
0.8
0.9
1
65
70
75
80
85
90

Fig.3(c)

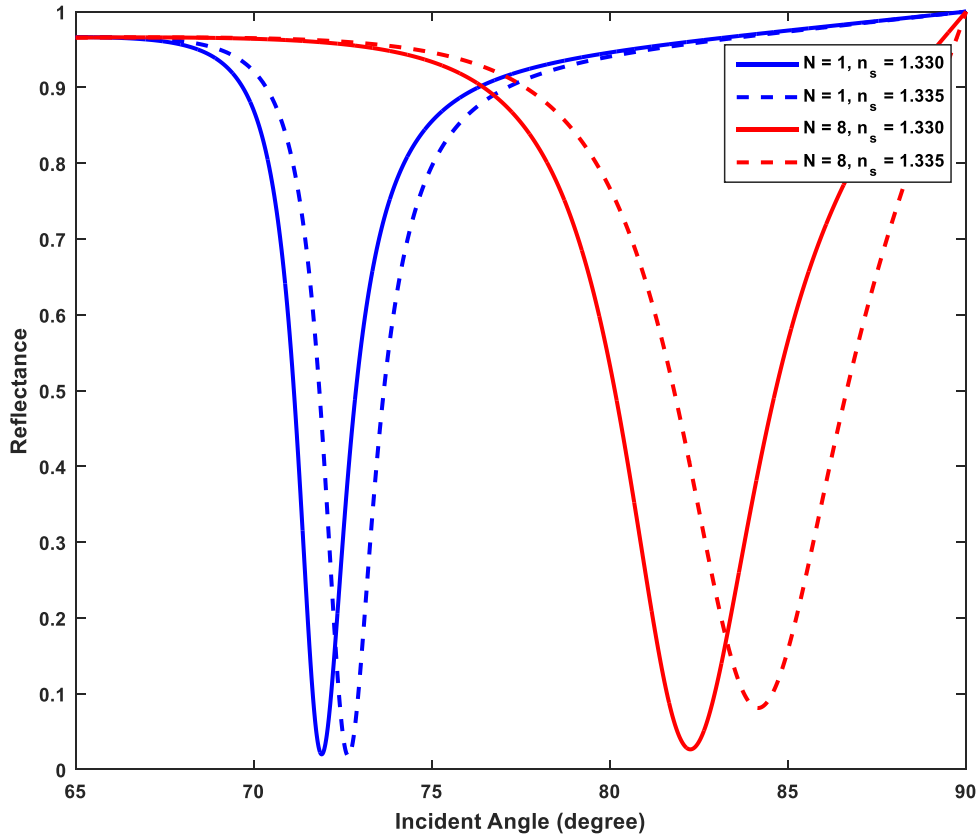

Reflectance
Incident Angle (degree)
N = 1, n_s = 1.330
N = 1, n_s = 1.335
N = 8, n_s = 1.330
N = 8, n_s = 1.335
0
0.1
0.2
0.3
0.4
0.5
0.6
0.7
0.8
0.9
1
65
70
75
80
85
90

Fig.3(d)

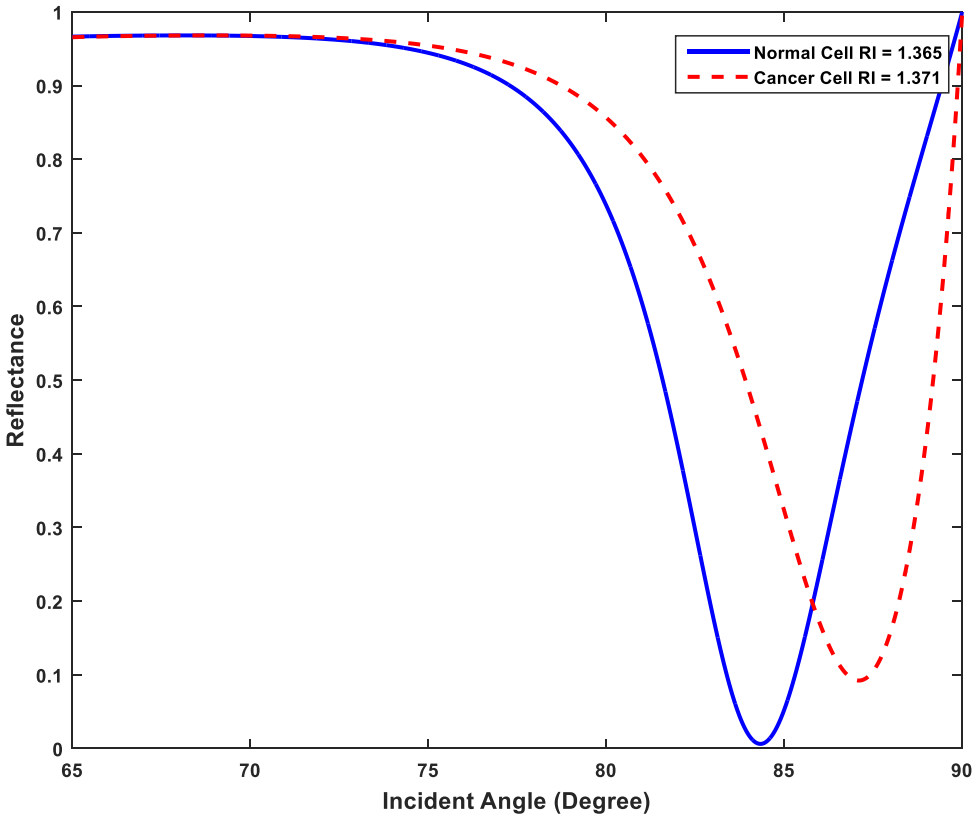

Normal Cell RI = 1.365
Cancer Cell RI = 1.371
Reflectance
Incident Angle (Degree)
0
0.1
0.2
0.3
0.4
0.5
0.6
0.7
0.8
0.9
1
65
70
75
80
85
90

Fig.4